

Theoretical analysis of co-solvent effect on the proton transfer reaction of glycine in a water–acetonitrile mixture

Yukako Kasai, Norio Yoshida,^{a)} and Haruyuki Nakano

Department of Chemistry, Graduate School of Sciences, Kyushu University, 6-10-1 Hakozaki, Higashi-ku, Fukuoka 812-8581, Japan

(Received 5 March 2015; accepted 11 May 2015; published online 26 May 2015)

The co-solvent effect on the proton transfer reaction of glycine in a water–acetonitrile mixture was examined using the reference interaction-site model self-consistent field theory. The free energy profiles of the proton transfer reaction of glycine between the carboxyl oxygen and amino nitrogen were computed in a water–acetonitrile mixture solvent at various molar fractions. Two types of reactions, the intramolecular proton transfer and water-mediated proton transfer, were considered. In both types of the reactions, a similar tendency was observed. In the pure water solvent, the zwitterionic form, where the carboxyl oxygen is deprotonated while the amino nitrogen is protonated, is more stable than the neutral form. The reaction free energy is $-10.6 \text{ kcal mol}^{-1}$. On the other hand, in the pure acetonitrile solvent, glycine takes only the neutral form. The reaction free energy from the neutral to zwitterionic form gradually increases with increasing acetonitrile concentration, and in an equally mixed solvent, the zwitterionic and neutral forms are almost isoenergetic, with a difference of only $0.3 \text{ kcal mol}^{-1}$. The free energy component analysis based on the thermodynamic cycle of the reaction also revealed that the free energy change of the neutral form is insensitive to the change of solvent environment but the zwitterionic form shows drastic changes. In particular, the excess chemical potential, one of the components of the solvation free energy, is dominant and contributes to the stabilization of the zwitterionic form. © 2015 AIP Publishing LLC. [<http://dx.doi.org/10.1063/1.4921432>]

I. INTRODUCTION

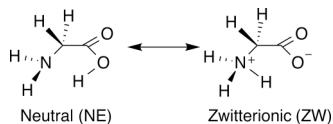
The co-solvent effect on chemical reactions has attracted a lot of attention in the field of chemistry, physics, and biochemistry. Most chemical reactions occurring in solution show drastic changes in character depending on the solvent environment. The solvent environment can be controlled by adding a co-solvent. Thus, binary mixtures, such as dimethylsulfoxide–water, methanol–water, and acetonitrile–water, have been explored as a reaction field or an analogue of the biological environment in both experimental and theoretical studies.^{1–6}

The proton transfer in binary mixtures has been of particular interest in biochemistry, because various proton transfers in biological systems usually occur in the heterogeneous medium.^{6–9} The zwitterionic–neutral (ZW–NE) proton transfer of glycine is a good probe to examine the co-solvent effect on the reaction (Scheme 1). The equilibrium of proton transfer reactions shifts depending on the ratio of the mixture. In the gas phase, glycine takes the NE form but not the ZW form.^{10–12} On the other hand, glycine takes ZW in polar solvents, such as water. By using the titration method, it has been clarified that the ZW of glycine is more stable than NE in water by $7.3 \text{ kcal mol}^{-1}$ in free energy.¹³ This is because the highly polarized ZW is unstable in the gas phase but is

strongly stabilized by the solute–solvent interaction in polar solvents.

To consider the co-solvent effect in binary mixtures on the proton transfer reaction, a useful tool is the reference interaction site model self-consistent field (RISM-SCF) method, which is a hybrid method of the quantum mechanics electronic structure theory and the statistical mechanics integral equation theory of molecular liquids.^{14–16} This method can treat the solvent effect on chemical reactions in solution at the molecular level by using RISM.¹⁷ The RISM-SCF and its extended version, the RISM-SCF spatial electron density distribution (RISM-SCF-SEDD), have been successfully applied to investigate various chemical and biological processes in mixtures of solvents. Hayaki *et al.* applied the RISM-SCF-SEDD method to a Diels–Alder reaction in ionic liquids¹⁸ and an S_N2 reaction in ionic liquids.¹⁹ They also applied this method to investigate the excited-state intramolecular proton transfer of 4′-N,N-diethylamino-3-hydroxyflavine in ionic liquids.²⁰ The free energy surface features of a proton transfer reaction obtained by their calculation were consistent with the experimental observations, and the computed absorption and emission energies also showed quantitative agreement with the experiments.^{21–23} The salt effect on chemical reactions has also been investigated by the RISM-SCF method with the concentration dependence of a Diels–Alder reaction in a LiCl solution. The concentration dependence on the activation barrier was in good agreement with that estimated experimentally.²⁴ Recently, we have reported an intramolecular proton transfer in a NaCl aqueous solution for a wide range of concentrations.²⁵ These studies

^{a)} Author to whom correspondence should be addressed. Electronic mail: noriwo@chem.kyushu-univ.jp. Telephone: +81-92-642-2588.



SCHEME 1. Scheme of intramolecular proton transfer between neutral and zwitterionic forms.

demonstrate the validity of the RISM-SCF method to investigate the co-solvent effect on the chemical processes in mixture solvents.

In the present study, we investigated the co-solvent effect on the intramolecular proton transfer reaction of glycine between NE and ZW in a water–acetonitrile mixture at various molar fractions. Two types of reaction are considered. One is the direct transfer of protons from carboxyl oxygen to amino nitrogen. The other is the solvent-mediated proton transfer reaction, where a solvent, water, mediates the reaction as both a proton donor and acceptor. We only examined one of the simplest cases of the solvent-mediated reaction proposed by Jensen and Gordon.¹⁰ In this case, only a single water molecule, which is located between the carboxyl oxygen and amino nitrogen, participates in the reaction.

We take the intrinsic reaction coordinate (IRC) as reaction coordinates of the proton transfer reactions in the solution. Along the reaction coordinates, the optimum structures of ZW and NE as well as the transition state (TS) structure are searched by using the analytical free energy gradient formula.¹⁶ The free energy change due to the change in the molar fraction of the mixture solvent is examined by free energy component analysis. The solvation structures of ZW and NE are also investigated to clarify the origin of the co-solvent effect.

II. METHOD

A. Brief overview of the method

We employed the RISM-SCF method for the free energy and geometry optimization calculations in solution.^{14–16} In the present study, we assume an infinite dilution of glycine into the water–acetonitrile mixture. With this assumption, the solute glycine is treated by quantum mechanics, and the surrounding solvent molecules, water and acetonitrile, are treated by the RISM method.

The Helmholtz energy A of the system is given by

$$A = E_{\text{solute}} + \Delta\mu, \quad (1)$$

where E_{solute} is the solute electronic energy and $\Delta\mu$ is the excess chemical potential due to the solvation. E_{solute} is computed from a quantum chemical electronic structure calculation,

$$E_{\text{solute}} = \langle \Psi | H_0 | \Psi \rangle, \quad (2)$$

where H_0 and Ψ are the electronic Hamiltonian of an isolated molecule and wave function of a solute molecule, respectively. In the RISM-SCF method, the excess chemical potential is given by

$$\Delta\mu = 4\pi \sum_v^{\text{Solvent species}} \rho_v k_B T \sum_\alpha^{\text{Solute site}} \sum_\gamma^{\text{Solvent site}} \int dr \left[\frac{1}{2} (h_{\alpha\gamma}(r))^2 \theta(h_{\alpha\gamma}(r)) - c_{\alpha\gamma}(r) - \frac{1}{2} h_{\alpha\gamma}(r) c_{\alpha\gamma}(r) \right] r^2. \quad (3)$$

Here, k_B , T , ρ_v , and θ are the Boltzmann constant, the absolute temperature, the number density of the solvent species v , and the Heaviside step function, respectively. The summation of v in right hand side is running over all solvent species, while the summation of γ is running over the solvent site belonging to the species v . $h_{\alpha\gamma}$ and $c_{\alpha\gamma}$ are the site–site total and direct correlation functions, respectively. To derive Eq. (3), we employed the Kovalenko-Hirata (KH) closure,^{26,27}

$$h_{\alpha\gamma}(r) = \begin{cases} \exp\{d_{\alpha\gamma}(r)\} - 1 & \text{for } d_{\alpha\gamma}(r) < 0 \\ d_{\alpha\gamma}(r) & \text{for } d_{\alpha\gamma}(r) \geq 0 \end{cases} \quad (4)$$

$$d_{\alpha\gamma}(r) = -\frac{1}{k_B T} u_{\alpha\gamma}(r) + h_{\alpha\gamma}(r) - c_{\alpha\gamma}(r),$$

where $u_{\alpha\gamma}$ is the interaction potential between the solute site α and solvent site γ ,

$$u_{\alpha\gamma}(r) = \frac{q_\alpha q_\gamma}{r} + 4\epsilon_{\alpha\gamma} \left[\left(\frac{\sigma_{\alpha\gamma}}{r} \right)^{12} - \left(\frac{\sigma_{\alpha\gamma}}{r} \right)^6 \right], \quad (5)$$

where q_α and q_γ denote the effective point charge on solute site α and solvent site γ , and $\epsilon_{\alpha\gamma}$ and $\sigma_{\alpha\gamma}$ are the Lennard-Jones parameter with usual meanings. The total and direct correlation functions are determined by solving Eq. (4) with the RISM equation,

$$h_{\alpha\gamma} = \omega_{\alpha\alpha'} * c_{\alpha'\gamma'} * \omega_{\gamma'\gamma} + \rho_{\gamma'} \omega_{\alpha\alpha'} * c_{\alpha'\gamma'} * h_{\gamma'\gamma}, \quad (6)$$

where $\omega_{\alpha\alpha'}$ is the intramolecular correlation function and $*$ denotes the convolution integral.

B. Computational details

The density functional theory with the M06-2X and B3LYP exchange-correlation functionals²⁸ was employed for the electronic structure calculation of solute glycine at 6-31G, 6-31+G(d), and 6-31++G(d,p) levels.

The RISM calculations were performed in the water–acetonitrile mixture at 298 K. The molar fractions of acetonitrile to the mixture solvent were selected as 0.00, 0.27, 0.50, 0.76, and 1.00. The number density of the components of the solution was determined computationally, where we assumed that the volumes of water and acetonitrile molecules were identical to those for the saturated solution. The Lennard-Jones parameters for solute amino acid and acetonitrile were taken from the all-atom optimized potential for liquid simulations (OPLS-AA) parameter set.²⁹ The simple point charge (SPC) model parameter set for the geometrical and potential parameters for the solvent water was employed with modified hydrogen parameters ($\sigma = 1.0 \text{ \AA}$ and $\epsilon = 0.056 \text{ kcal mol}^{-1}$). The grid points in the RISM-SCF calculation were 2048 with a spacing of 0.01 \AA .

In order to determine the effective point charge on solute site α , q_α , we employed the restraint electrostatic potential (RESP) method with the geodesic point selection scheme.^{30,31} The restraint parameter for the harmonic penalty function was

TABLE I. The functional and basis set dependence of the reaction free energy in pure water (in kcal mol⁻¹).

| Functional | Basis set | ΔA | ΔA^\ddagger |
|--------------------------|--------------|------------|---------------------|
| M06-2X | 6-31G | -10.50 | 0.12 |
| | 6-31+G(d) | -12.93 | 2.08 |
| | 6-31++G(d,p) | -10.62 | 1.22 |
| B3LYP | 6-31G | -10.58 | 0.06 |
| | 6-31+G(d) | -15.23 | 1.31 |
| | 6-31++G(d,p) | -13.23 | 0.93 |
| CPMD ¹² | | -11.2 | 1.5 |
| QM/MM-MD ¹¹ | | -13.9 | 1.8 |
| Experiment ¹³ | | -7.27 | NA |

chosen as 0.003. For the point selection, the scale factor for the first shell of van der Waals spheres, the increment for successive shells, and number of layers of points were chosen as 1.2, 0.1, and 10, respectively. With these parameters, approximately 2600 points were selected for RESP fitting.

The free energy calculations were conducted along the reaction coordinates determined by the IRC method in solution.

All the calculations were performed with a modified version of the GAMESS program package,³² where the RISM-SCF method and its energy gradient method have been implemented.^{33,34}

III. RESULTS AND DISCUSSION

We examined two types of reaction paths of a glycine proton transfer from NE to ZW in the water–acetonitrile mixture. One is the intramolecular proton transfer. In this type, the proton transfers directly from the carboxyl oxygen to the amino nitrogen. The other is the water-mediated proton transfer. This type comprises two simultaneous proton transfers, where a solvent water gets a proton from the carboxyl oxygen and simultaneously gives another proton to the amino nitrogen of glycine.

A. Assessment of the exchange-correlation functional and basis functions

We first examined the functional and basis function dependencies of the reaction free energy and the activation free energy of the intramolecular proton transfer reaction from NE to ZW in pure water. In Table I, the computed reaction free

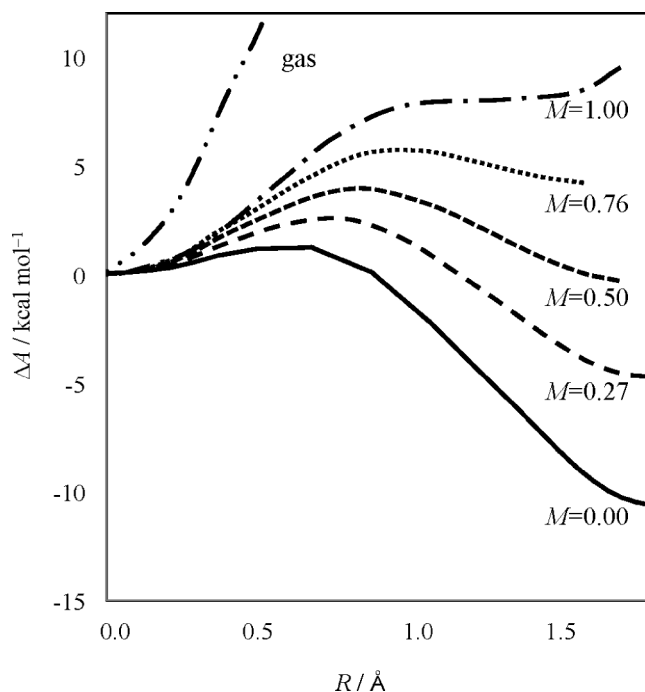


FIG. 1. The free energy changes from NE to ZW. Insets of the figure, M , denote the molar fraction of acetonitrile in the solvent.

energy and the activation free energy are summarized. The reaction free energy ΔA is defined as follows:

$$\Delta A = A^{\text{ZW}} - A^{\text{NE}}, \quad (7)$$

where A^{ZW} and A^{NE} are the free energies at ZW and NE. Similarly, the activation free energy ΔA^\ddagger is defined by

$$\Delta A^\ddagger = A^{\text{TS}} - A^{\text{NE}}, \quad (8)$$

where A^{TS} is the free energy at TS.

As can be seen in the table, both the free energies strongly depend on the basis functions whereas the functional dependence is relatively small, which is in accord with the results reported by Kido *et al.*³⁵ Although the computed reaction free energies are overestimated to the experimental value, -7.27 kcal mol⁻¹, M06-2X/6-31++G(d,p) calculation shows comparable values with the experiment. The reaction free energy and the activation free energy are also in good agreement with those by Car-Parrinello molecular dynamics results by Leung and Rempe.¹² Most recently, Takenaka *et al.* applied quantum mechanics/molecular mechanics molecular

TABLE II. The reaction free energy, the activation free energy, and key bond lengths. The units of free energy and bond length are kcal mol⁻¹ and Å, respectively.

| Molar fraction | ZW | | TS | | NE | | ΔA | ΔA^\ddagger |
|--------------------|-----------------|-----------------|-----------------|-----------------|-----------------|-----------------|------------|---------------------|
| | $R(\text{N-H})$ | $R(\text{O-H})$ | $R(\text{N-H})$ | $R(\text{O-H})$ | $R(\text{N-H})$ | $R(\text{O-H})$ | | |
| $M = 0.00$ (water) | 1.04 | 2.01 | 1.34 | 1.18 | 1.84 | 1.00 | -10.62 | 1.29 |
| $M = 0.27$ | 1.04 | 1.96 | 1.29 | 1.23 | 1.85 | 1.00 | -4.70 | 2.61 |
| $M = 0.50$ | 1.04 | 1.88 | 1.24 | 1.28 | 1.85 | 0.99 | -0.29 | 3.91 |
| $M = 0.76$ | 1.06 | 1.77 | 1.19 | 1.35 | 1.86 | 0.99 | 4.18 | 5.70 |
| $M = 1.00$ | ... | ... | ... | ... | 1.87 | 0.99 | ... | ... |
| Gas | ... | ... | ... | ... | 1.94 | 0.98 | ... | ... |

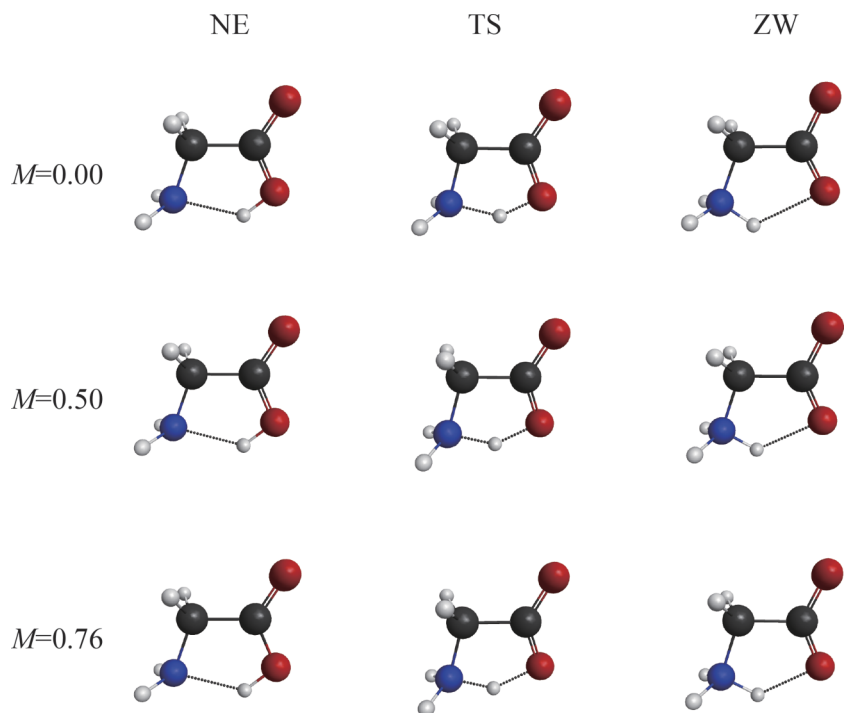


FIG. 2. The optimized structures of glycine for NE, TS, and ZW in $M = 0.00, 0.50,$ and 0.76 .

TABLE III. The free energy components of the reaction (in kcal mol⁻¹).

| Molar fraction | ΔA | $\Delta E_{\text{gas}}^{\text{ZW-NE}}$ | $\Delta E_{\text{dist}}^{\text{ZW}}$ | $\Delta E_{\text{dist}}^{\text{NE}}$ | $\Delta \mu^{\text{ZW}}$ | $\Delta \mu^{\text{NE}}$ |
|--------------------|------------|--|--------------------------------------|--------------------------------------|--------------------------|--------------------------|
| $M = 0.00$ (water) | -10.62 | 27.18 | 24.80 | 8.95 | -61.65 | -7.99 |
| $M = 0.27$ | -4.70 | 25.96 | 15.32 | 5.23 | -47.48 | -6.73 |
| $M = 0.50$ | -0.29 | 24.49 | 10.11 | 6.21 | -36.41 | -4.93 |
| $M = 0.76$ | 4.18 | 22.75 | 6.01 | 2.01 | -25.45 | -2.88 |
| $M = 1.00$ | ... | ... | ... | 1.11 | ... | -1.14 |

TABLE IV. The atomic components of excess chemical potential difference between NE and ZW (in kcal mol⁻¹).

| Solute atom x | $M = 0.00$ | | $M = 0.27$ | | $M = 0.50$ | | $M = 0.76$ | |
|-----------------|--|--|--|--|--|--|--|--|
| | $\Delta \Delta \mu_{x, \text{H}_2\text{O}}^{\text{ZW-NE}}$ | $\Delta \Delta \mu_{x, \text{CH}_3\text{CN}}^{\text{ZW-NE}}$ | $\Delta \Delta \mu_{x, \text{H}_2\text{O}}^{\text{ZW-NE}}$ | $\Delta \Delta \mu_{x, \text{CH}_3\text{CN}}^{\text{ZW-NE}}$ | $\Delta \Delta \mu_{x, \text{H}_2\text{O}}^{\text{ZW-NE}}$ | $\Delta \Delta \mu_{x, \text{CH}_3\text{CN}}^{\text{ZW-NE}}$ | $\Delta \Delta \mu_{x, \text{H}_2\text{O}}^{\text{ZW-NE}}$ | $\Delta \Delta \mu_{x, \text{CH}_3\text{CN}}^{\text{ZW-NE}}$ |
| N1 | 4.5 | ... | 1.8 | -3.8 | 0.6 | -3.4 | 0.2 | -4.7 |
| H2 | -5.3 | ... | -3.1 | -0.6 | -1.3 | -1.5 | -0.3 | -1.6 |
| H3 | -6.1 | ... | -3.1 | -0.5 | -1.9 | -1.9 | -0.7 | -2.3 |
| H4 | -5.9 | ... | -3.0 | -0.5 | -1.9 | -1.8 | -0.7 | -2.3 |
| C5 | -2.3 | ... | -0.8 | -0.2 | -0.5 | 0.7 | -0.3 | 1.3 |
| C6 | 18.9 | ... | 10.4 | 0.7 | 7.9 | 1.2 | 3.9 | 2.2 |
| O7 | -25.1 | ... | -15.7 | -0.9 | -11.1 | -2.0 | -5.3 | -3.3 |
| O8 | -33.3 | ... | -20.2 | -0.1 | -13.5 | -0.8 | -6.2 | -2.1 |
| H9 | 0.4 | ... | 0.2 | 0.0 | 0.2 | -0.3 | 0.1 | -0.4 |
| H10 | 0.4 | ... | 0.2 | 0.0 | 0.2 | -0.3 | 0.1 | -0.4 |

dynamics simulation with MP2/6-31+G(d).¹¹ Their results are similar to the M06-2X/6-31+G(d) results of the present study.

Hereafter, we only employ M06-2X/6-31++G(d,p) for detailed analysis from its validity.

B. Free energy profile for the intramolecular proton transfer

We examined the free energy profile of the intramolecular proton transfer reaction from NE to ZW in the water-

acetonitrile mixture. The computed molar fraction of acetonitrile in the mixture solvent was 0.00, 0.27, 0.50, 0.76, and 1.00. We also made a profile in the gas phase for comparison.

In Figure 1, the free energy changes are depicted along the reaction coordinate from NE to ZW. The reaction free energy and the activation free energy are summarized in Table II. We have selected the difference of the N-H and O-H bond lengths, $R(\text{N-H}) - R(\text{O-H})$, as the reaction coordinate R , where $R(\text{N-H})$ and $R(\text{O-H})$ are the distances between the amino

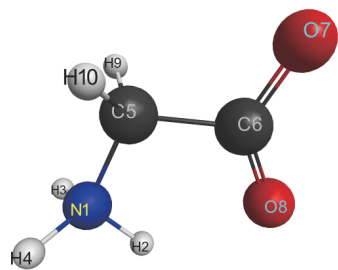


FIG. 3. Numbering for the solute atoms.

nitrogen and proton and between the carboxyl oxygen and proton, respectively.

In the gas phase, TS and ZW were not located; the free energy increases monotonically from NE. This is because the localized electron distribution destabilizes ZW in the gas phase. On the other hand, in the pure water solvent, $M = 0.00$, ZW is more stable than NE, with both ZW and NE located as locally stable structures. The free energy of ZW is $10.6 \text{ kcal mol}^{-1}$ lower than that of NE, and the activation free energy is $1.3 \text{ kcal mol}^{-1}$. As the molar fraction of acetonitrile in the mixture solvent increases, the reaction free

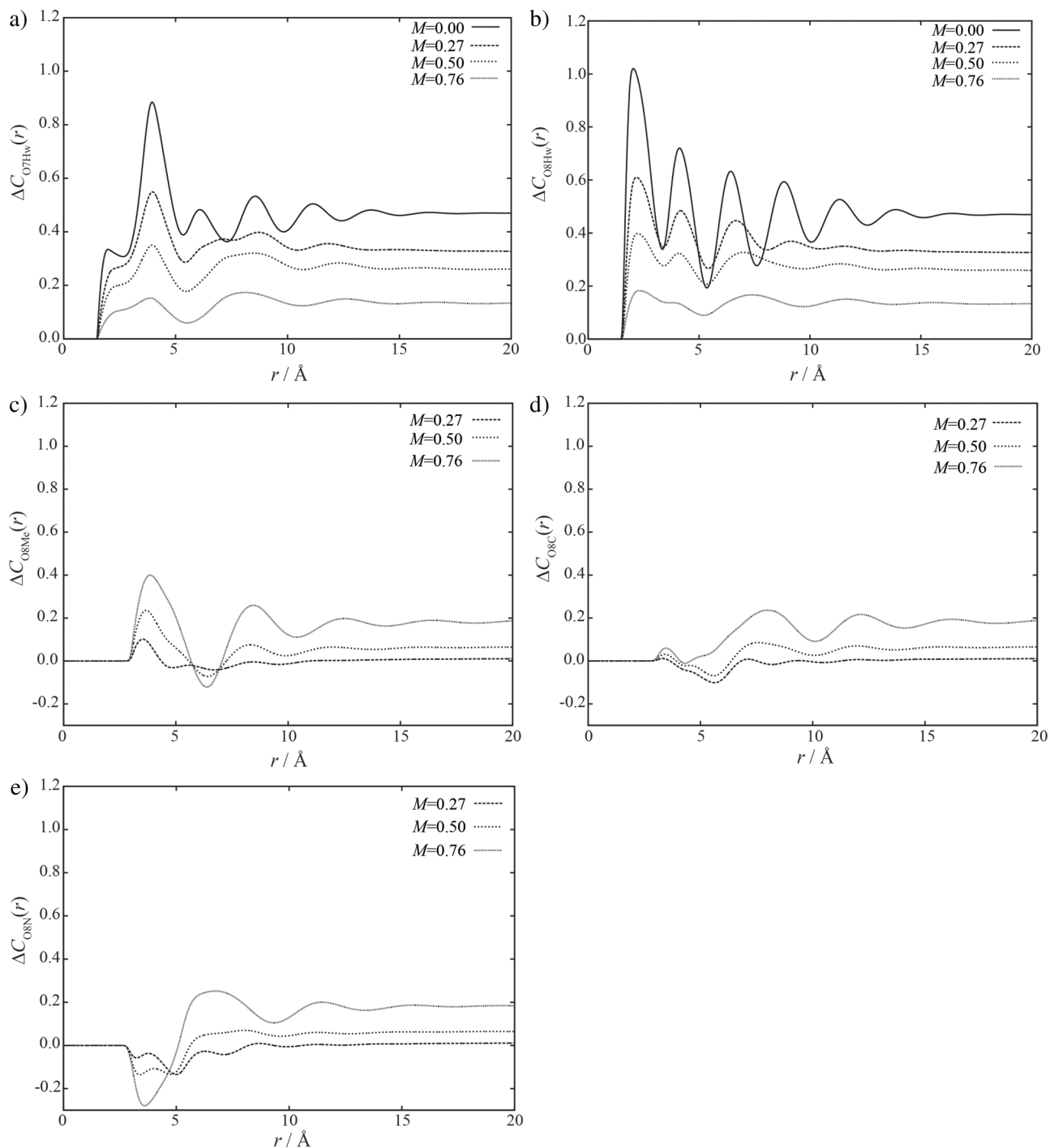


FIG. 4. Relative coordination number from NE to ZW of (a) solvent water hydrogen H_w for solute carbonyl oxygen O7, (b) H_w for O7, (c) solvent acetonitrile methyl group Me for O8, (d) acetonitrile cyanocarbon C for O8, and (e) cyanonitrogen N for O8.

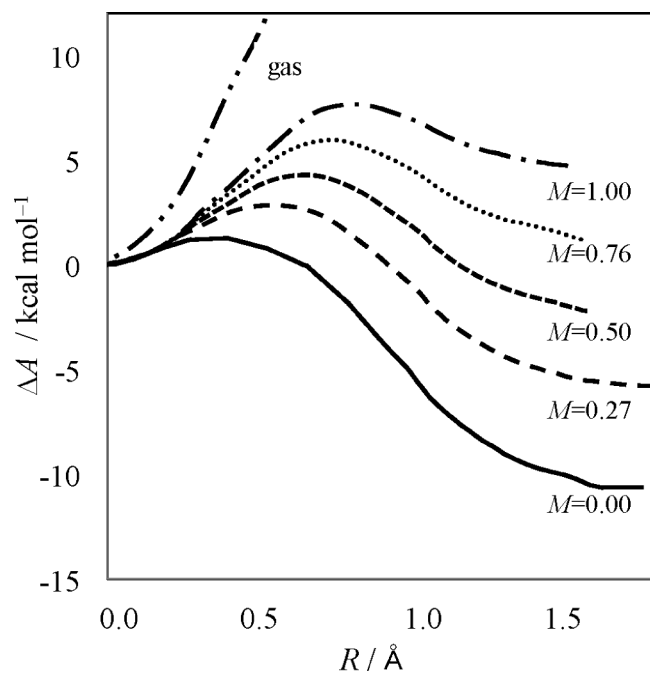


FIG. 5. Free energy change from NE to ZW for the one-water-mediated proton transfer. Insets of the figure, M , denote the molar fraction of acetonitrile of the solvent.

energy increases, namely, -4.70 , -0.29 , and 4.18 kcal mol $^{-1}$ for a molar fraction of 0.27 , 0.50 , and 0.76 , respectively. In an equally mixed solvent, ZW and NE become almost isoenergetic with the difference being only 0.3 kcal mol $^{-1}$. ZW does not have a locally stable structure in pure acetonitrile solvent, $M = 1.00$, and the profile exhibited a similar behavior to that in the gas phase. In accordance with the behavior of the reaction free energy, the activation free energy of the reaction increases as the molar fraction increases, namely, 2.61 , 3.91 , and 5.70 kcal mol $^{-1}$ for a molar fraction of 0.27 , 0.50 , and 0.76 , respectively.

The optimized structures of NE, TS, and ZW are shown in Figure 2, and $R(\text{N-H})$ and $R(\text{O-H})$ of each structure are summarized in Table II. For NE and ZW, $R(\text{N-H})$ becomes longer as the molar fraction of acetonitrile increases whereas $R(\text{O-H})$ gets shorter. It means that the structures of NE and ZW come close to the NE structure in the gas phase when increasing the molar fraction of acetonitrile. The $R(\text{N-H})$ decreases whilst $R(\text{O-H})$ increases with increasing acetonitrile molar fraction at TS. Thus, the structural features of TS come close to ZW.

TABLE V. Key bond lengths, reaction free energy, and activation free energy for the one-water-mediated proton transfer reaction. The units of bond length and free energy are kcal mol $^{-1}$ and Å, respectively.

| Molar fraction | ZW | | | TS | | | NE | | | ΔA | ΔA^\ddagger |
|----------------|------------------|------------------|-------------------|------------------|------------------|-------------------|------------------|------------------|-------------------|------------|---------------------|
| | $R(\text{N-H2})$ | $R(\text{O-H2})$ | $R(\text{O-H13})$ | $R(\text{N-H2})$ | $R(\text{O-H2})$ | $R(\text{O-H13})$ | $R(\text{N-H2})$ | $R(\text{O-H2})$ | $R(\text{O-H13})$ | | |
| $M = 0.00$ | 1.06 | 2.26 | 2.25 | 1.46 | 2.53 | 1.22 | 1.67 | 2.62 | 1.03 | -10.65 | 1.26 |
| $M = 0.27$ | 1.05 | 2.43 | 2.16 | 1.38 | 2.53 | 1.27 | 1.71 | 2.65 | 1.02 | -5.78 | 2.82 |
| $M = 0.50$ | 1.05 | 2.52 | 1.96 | 1.32 | 2.53 | 1.28 | 1.74 | 2.67 | 1.01 | -2.06 | 4.85 |
| $M = 0.76$ | 1.05 | 2.54 | 1.86 | 1.28 | 2.52 | 1.27 | 1.76 | 2.70 | 1.01 | 1.19 | 5.94 |
| $M = 1.00$ | 1.05 | 2.56 | 1.78 | 1.23 | 2.53 | 1.28 | 1.78 | 2.72 | 1.00 | 4.73 | 7.64 |
| Gas | ... | ... | ... | ... | ... | ... | 1.86 | 2.81 | 0.99 | ... | ... |

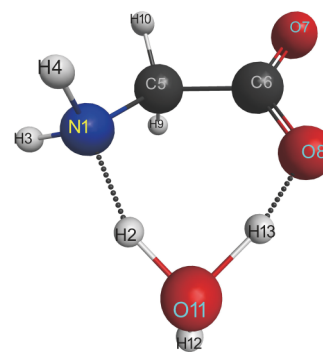


FIG. 6. Transition state structure with the numbering of atoms for the one-water-mediated proton transfer reaction.

These features are also seen in Figure 1. The position of TS on the reaction coordinate shifts to the ZW side when increasing the acetonitrile molar fraction.

In order to elucidate the origin of the behavior, we performed a solvation free energy decomposition analysis. By taking a thermodynamic cycle of the reaction, the change of the Helmholtz energy A from the reactant, ΔA , given in Eq. (7), can be rewritten as

$$\Delta A = \Delta E_{\text{gas}}^{\text{ZW-NE}} + \Delta E_{\text{dist}}^{\text{ZW}} - \Delta E_{\text{dist}}^{\text{NE}} + \Delta \mu^{\text{ZW}} - \Delta \mu^{\text{NE}}. \quad (9)$$

Here, $\Delta E_{\text{gas}}^{\text{ZW-NE}}$ is the reaction energy in the gas phase. ΔE_{dist} is the electronic distortion energy by solvation, defined as follows:

$$\Delta E_{\text{dist}} = E_{\text{solute}} - E_{\text{gas}}, \quad (10)$$

where E_{gas} is the gas phase energy of glycine with its geometry optimized in solution. In Table III, the free energy components present in Eq. (9) are summarized. The reaction energy in the gas phase, $\Delta E_{\text{gas}}^{\text{ZW-NE}}$, decreases with increasing the acetonitrile molar fraction. As seen in Figures 1 and 2, ZW comes close to NE on the reaction coordinate. Those smaller structural changes may contribute to smaller changes in $\Delta E_{\text{gas}}^{\text{ZW-NE}}$. Both in NE and ZW, the electronic distortion energy decreases and the excess chemical potential increases when increasing the acetonitrile molar fraction. These results indicate that the solute-solvent interaction becomes weaker by addition of acetonitrile. In the case of NE, the excess chemical potential and the electronic distortion energy compensate each other, which makes the sum of these values around zero, $|\Delta E_{\text{dist}}^{\text{NE}} - \Delta \mu^{\text{NE}}| < 1.5$ kcal mol $^{-1}$ for all the molar fractions. On

the other hand, ZW shows remarkable changes in excess chemical potential and electronic distortion energy. In particular, the excess chemical potential is dominant and largely contributes to the stabilization of ZW. This means that the strong solute–solvent electronic interactions give a negative excess chemical potential, and the electronic structural changes due to the solute–solvent interaction cause positive distortion energy.

From these results, we can say that the major factor of stabilizing ZW is the excess chemical potential rather than the electronic distortion energy. To then get microscopic information on the solvation structure, we examined the atomic components of excess chemical potential. The excess chemical potential, Eq. (3), can be decomposed into the contribution from the solute atoms, $\Delta\mu_{x,v}$,

$$\Delta\mu = \sum_v^{\text{solvent}} \sum_x^{\text{solute atom}} \Delta\mu_{x,v}, \quad (11)$$

from which we can see how each atom contributes to the stabilization or destabilization by solvation. The difference of the atomic components of excess chemical potential between NE and ZW, $\Delta\Delta\mu_{x,v}^{\text{ZW-NE}} = \Delta\mu_{x,v}^{\text{ZW}} - \Delta\mu_{x,v}^{\text{NE}}$, is summarized in Table IV, where $\Delta\mu_{x,v}^{\text{ZW}}$ and $\Delta\mu_{x,v}^{\text{NE}}$ denote the atomic components of excess chemical potential of solute atom x coming from solvent v at ZW and NE, respectively. The labels of the solute atoms are defined in Figure 3. In pure water, $M = 0.00$, the components of two carboxyl oxygen atoms, O7 and O8, contribute to the stabilization of ZW, whereas the amino nitrogen and the carboxyl carbon destabilize ZW. Increasing the acetonitrile molar fraction, the solvent effect of water drastically weakens whereas that of acetonitrile gets marginally stronger. For instance, $\Delta\Delta\mu_{\text{O8,H}_2\text{O}}^{\text{ZW-NE}}$ changes by 27.1 kcal mol⁻¹ from $M = 0.0$ to 0.76, but $\Delta\Delta\mu_{\text{O8,CH}_3\text{CN}}^{\text{ZW-NE}}$ changes by only

−2.1 kcal mol⁻¹. Thus, the contribution from the water dominates the solvent effect on the proton transfer reaction.

The change of the excess chemical potential is related to the solvation structural changes from NE to ZW. To see the solvation structural changes, we defined the relative coordination numbers (RCNs),

$$\Delta C_{\alpha\gamma}(r) = C_{\alpha\gamma}^{\text{ZW}}(r) - C_{\alpha\gamma}^{\text{NE}}(r), \quad (12)$$

where $C_{\alpha\gamma}(r)$ is the running coordination number of solvent site γ around solute site α , defined by

$$C_{\alpha\gamma}(r) = 4\pi\rho_\gamma \int_0^r s^2 g_{\alpha\gamma}(s) ds. \quad (13)$$

RCNs indicate the degree of change in number of solvent atoms around a solute atom from NE to ZW.

In Figures 4(a) and 4(b), the RCNs of solvent water hydrogen H_w for solute carboxyl oxygen O7 and O8, namely, ΔC_{O7H_w} and ΔC_{O8H_w} , in various mixture ratios are depicted. Charges on O7 and O8 are induced by the polarization due to proton transfer. For instance, in pure water, the point charge on O7 and O8 changes from NE −0.84 and −0.57 to ZW −1.02 and −0.97, respectively. As a consequence, the attractive force between the solute carboxyl oxygen and solvent hydrogens is induced, and hence the RCNs show positive value. For both O7 and O8, the height of RCNs decreases when decreasing the molar fraction of water. In the case of O8, the conspicuous peaks at around 2 Å are observed whereas the corresponding peaks are small for O7. Because the protonated state of the O8 changes due to proton transfer, the coordination number of water hydrogen shows a drastic change. In Figures 4(c)–4(e), the RCN of solvent acetonitrile for O8 is shown. Because the cyanocarbon is located at the center of the solvent molecule,

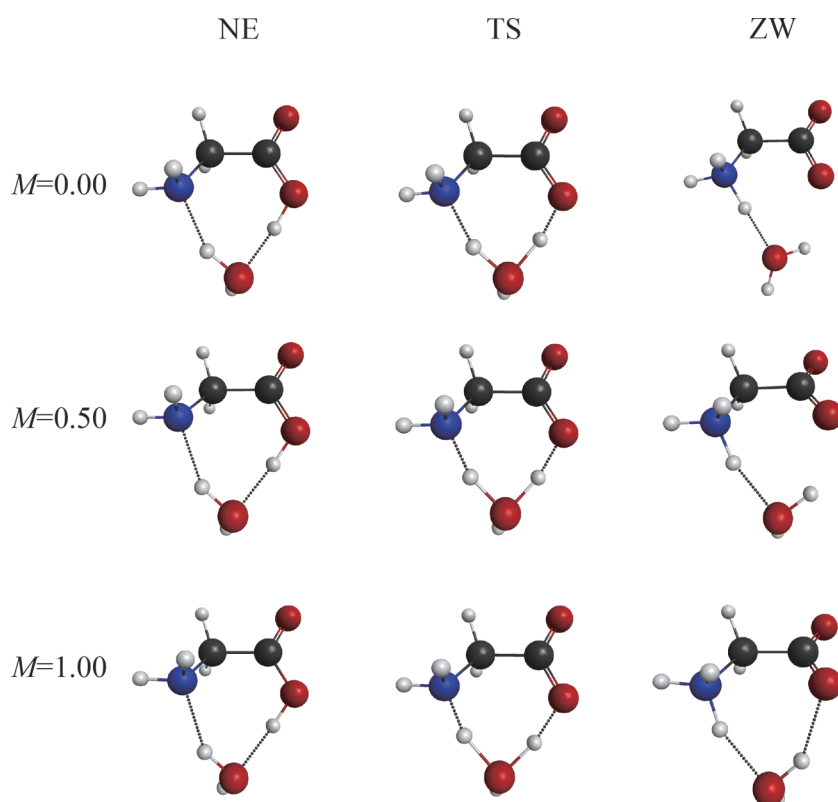


FIG. 7. The optimized structures of glycine-water complex for NE, TS, and ZW in $M = 0.00$, 0.50, and 1.00.

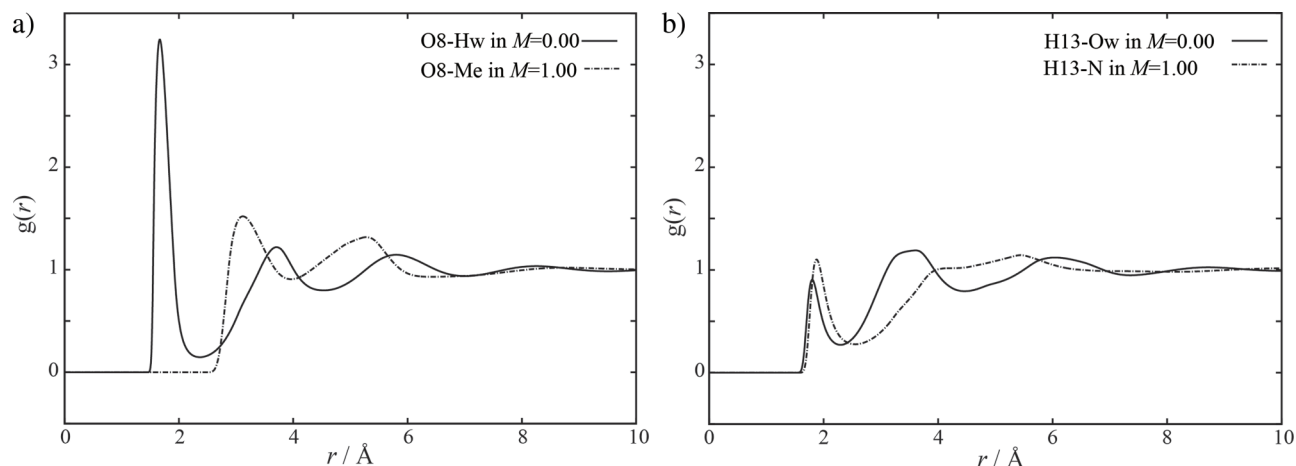


FIG. 8. The radial distribution functions between (a) solute O8 of ZW form and solvent and (b) solute H13 of ZW form and solvent.

the solvation structure is insensitive to the change of the solute form; hence, why the 1st peaks of RCNs are small. The RCNs of the methyl group and the cyanonitrogen show opposite behavior because the point charges on the cyanonitrogen and the methyl group have an opposite sign. ΔC_{O8Me} is enhanced positively but ΔC_{O8N} is enhanced negatively by increasing the acetonitrile concentration. The peak height of RCNs of acetonitrile is smaller and the position of the 1st peak is more departed from the solute atom, compared with those of water. This is because the contribution from acetonitrile to the stabilization is smaller than that from water.

C. Free energy profile for the one-water-mediated proton transfer

In the proton transfer reaction in aqueous solution, the solvent water is expected to mediate the reaction as a proton donor and acceptor. We examined the free energy profile of the water-mediated reaction in water–acetonitrile mixtures at various molar fractions of acetonitrile. It is noted that the molar fractions used in this subsection are not exactly the same as those in Subsection III B because one extra water exists in the system as a solute. The reaction path of the water-mediated proton transfer is highly complicated, because one or more solvent waters can participate in the reaction. In the present study, we only examined the simplest case of the reaction as proposed by Jensen and Gordon.²⁸ In this case, only a single water molecule is located between the carboxyl oxygen and amino nitrogen and participates in the reaction.

The free energy changes along the reaction coordinate are depicted in Figure 5. Similar trends to those in the intramolecular reaction are observed. When comparing the same molar fractions as the intramolecular reaction, the one-water-mediated reaction has a slightly larger magnitude of reaction free energy, ΔA , and activation free energy, ΔA^\ddagger , in most cases. The differences in activation free energy and reaction free energy from the case of the intramolecular proton transfer become larger when increasing the acetonitrile concentration. For instance, the difference of reaction free energy in pure water is only $0.03 \text{ kcal mol}^{-1}$ but is $2.99 \text{ kcal mol}^{-1}$ in $M = 0.76$ solution. In the pure acetonitrile solution, $M = 1.00$, the stable structure of ZW is located, which is not observed in

the case of intramolecular proton transfer. This indicates that only one water is enough to stabilize ZW in the acetonitrile.

Some key bond lengths are summarized in Table V. The labels of hydrogen atoms in the table are defined in Figure 6. The structural parameters of ZW strongly depend on the acetonitrile concentration, whereas those of NE do not, showing only small changes. The change in $R(\text{O}–\text{H13})$ of ZW is -0.47 \AA from $M = 0.00$ to $M = 1.00$. In Figure 7, some selected structures of the glycine–water complex are shown. Although NE shows close structures in $M = 0.00$ and $M = 1.00$, the ZW structure in $M = 0.00$ and $M = 1.00$ shows different hydrogen-bond networks between glycine and the “mediating water.” In Figures 8(a) and 8(b), the radial distribution functions (RDFs) of the solvent atoms for O8 and H13 are depicted, respectively. The RDF for solute O8 shows a conspicuous peak of a water hydrogen at around 1.8 \AA , while the peak of the acetonitrile methyl group at around 3 \AA is low. This indicates that O8 forms a hydrogen bond with the solvent water hydrogen in $M = 0.00$. However, O8 forms it with the mediating water in $M = 1.00$ because no hydrogen donor exists in the solvent. Figure 8(b) indicates that one of the hydrogens of the mediating water, H13, orients to the bulk and forms a hydrogen bond with a solvent water in $M = 0.00$ and acetonitrile $M = 1.00$.

IV. CONCLUSION

We have investigated the co-solvent effect on the proton transfer reaction of glycine in a water–acetonitrile mixture using RISM-SCF theory.

We first examined the intramolecular proton transfer reaction. The free energy profiles were computed at various ratios of acetonitrile molar fractions and were analyzed in detail. The set of profiles clearly showed that, with increasing concentrations of acetonitrile, ZW destabilizes and the activation free energy of the reaction heightens. From the energy decomposition analysis of the free energy of solvation, we found that a major factor stabilizing ZW is the strong solute–solvent electronic interactions rather than the energy of the structural change. From the RDFs, we also found that as the acetonitrile concentration increases, the hydrogen bond between the amino oxygen and solvent hydrogen becomes weak whilst ZW becomes unstable.

We also considered the one-water-mediated intermolecular proton transfer reaction. The molar fraction dependence of the free energy profile was similar to that of the intramolecular reaction. The free energy change and the activation energy of the reaction were slightly larger, and the structures and the solvent distribution were almost the same as those of the intramolecular reaction. The position of the mediating water in ZW was quite different from that in pure water and in pure acetonitrile. The carboxyl oxygen forms hydrogen bonds with a solvent water in pure water whereas it forms with the mediating water in pure acetonitrile because no hydrogen donor that exists is in pure acetonitrile solvent.

The detailed analysis of the co-solvent effect on the proton transfer reaction presented here should be indispensable for a deeper understanding of the solvation of amino acids in heterogeneous environments.

ACKNOWLEDGMENTS

Numerical calculations were partly conducted in the Research Center for Computational Science, Institute for Molecular Science, National Institutes of Natural Science. We would like to thank the Next Generation Supercomputing Project, Nanoscience Program and the Strategic Programs for Innovative Research (SPIRE) and the Computational Materials Science Initiative (CMSI), Japan, for their support. We are also grateful for Kyushu University Interdisciplinary Programs in Education and Projects in Research Development, and a Grant-in-Aid (Grant Nos. 25410021 and 26104526) from MEXT, Japan.

¹K. Gekko, E. Ohmae, K. Kameyama, and T. Takagi, *Biochim. Biophys. Acta, Protein Struct. Mol. Enzymol* **1387**, 195 (1998).

²S. Banerjee, S. Roy, and B. Bagchi, *J. Phys. Chem. B* **114**, 12875 (2010).

³T. Yamazaki, A. Kovalenko, V. V. Murashov, and G. N. Patey, *J. Phys. Chem. B* **114**, 613 (2010).

⁴A. A. Freitas, F. H. Quina, and A. A. Macanita, *J. Phys. Chem. A* **115**, 10988 (2011).

⁵S. Chatteraj, R. Chowdhury, S. Ghosh, and K. Bhattacharyya, *J. Chem. Phys.* **138**, 214507 (2013).

⁶J. Kuchlyan, D. Banik, A. Roy, N. Kundu, and N. Sarkar, *J. Phys. Chem. B* **118**, 13946 (2014).

⁷D. Zhong, A. Douhal, and A. H. Zewail, *Proc. Natl. Acad. Sci. U. S. A.* **97**, 14056 (2000).

⁸B. Cohen, C. M. Alvarez, N. A. Carmona, J. A. Organero, and A. Douhal, *J. Phys. Chem. B* **115**, 7637 (2011).

⁹A. Douhal, *Acc. Chem. Res.* **37**, 349 (2004).

¹⁰J. H. Jensen and M. S. Gordon, *J. Am. Chem. Soc.* **117**, 8159 (1995).

¹¹N. Takenaka, Y. Kitamura, Y. Koyano, T. Asada, and M. Nagaoka, *Theor. Chem. Acc.* **130**, 215 (2011).

¹²K. Leung and S. B. Rempe, *J. Chem. Phys.* **122**, 184506 (2005).

¹³G. Wada, E. Tamura, M. Okina, and M. Nakamura, *Bull. Chem. Soc. Jpn.* **55**, 3064 (1982).

¹⁴S. Ten-No, F. Hirata, and S. Kato, *Chem. Phys. Lett.* **214**, 391 (1993).

¹⁵S. Ten-No, F. Hirata, and S. Kato, *J. Chem. Phys.* **100**, 7443 (1994).

¹⁶H. Sato, F. Hirata, and S. Kato, *J. Chem. Phys.* **105**, 1546 (1996).

¹⁷F. Hirata, *Molecular Theory of Solvation* (Kluwer, Dordrecht, 2003).

¹⁸S. Hayaki, K. Kido, D. Yokogawa, H. Sato, and S. Sakaki, *J. Phys. Chem. B* **113**, 8227 (2009).

¹⁹S. Hayaki, K. Kido, H. Sato, and S. Sakaki, *Phys. Chem. Chem. Phys.* **12**, 1822 (2010).

²⁰S. Hayaki, Y. Kimura, and H. Sato, *J. Phys. Chem. B* **117**, 6759 (2013).

²¹M. Fukuda, M. Terazima, and Y. Kimura, *Chem. Phys. Lett.* **463**, 364 (2008).

²²Y. Kimura, M. Fukuda, K. Suda, and M. Terazima, *J. Phys. Chem. B* **114**, 11847 (2010).

²³K. Suda, M. Terazima, and Y. Kimura, *Chem. Phys. Lett.* **531**, 70 (2012).

²⁴N. Yoshida, H. Tanaka, and F. Hirata, *J. Phys. Chem. B* **117**, 14115 (2013).

²⁵Y. Kasai, N. Yoshida, and H. Nakano, *J. Mol. Liq.* **200**, 32 (2014).

²⁶A. Kovalenko and F. Hirata, *J. Chem. Phys.* **110**, 10095 (1999).

²⁷A. Kovalenko and F. Hirata, *Chem. Phys. Lett.* **349**, 496 (2001).

²⁸Y. Zhao and D. G. Truhlar, *Theor. Chem. Acc.* **120**, 215 (2008).

²⁹W. L. Jorgensen, D. S. Maxwell, and J. TiradoRives, *J. Am. Chem. Soc.* **118**, 11225 (1996).

³⁰M. Spackman, *J. Comput. Chem.* **17**, 1 (1996).

³¹C. Bayly, P. Cieplak, W. Cornell, and P. Kollman, *J. Phys. Chem.* **97**, 10269 (1993).

³²M. W. Schmidt, K. K. Baldrige, J. A. Boatz, S. T. Elbert, M. S. Gordon, J. H. Jensen, S. Koseki, N. Matsunaga, K. A. Nguyen, S. Su, T. L. Windus, M. Dupuis, and J. A. Montgomery, *J. Comput. Chem.* **14**, 1347 (1993).

³³N. Yoshida and F. Hirata, *J. Comput. Chem.* **27**, 453 (2006).

³⁴N. Yoshida, Y. Kiyota, and F. Hirata, *J. Mol. Liq.* **159**, 83 (2011).

³⁵K. Kido, H. Sato, and S. Sakaki, *Int. J. Quantum Chem.* **112**, 103 (2012).